



NANOSTRUCTURED LIPID CARRIERS AS A PROMISING DERMAL DELIVERY PLATFORM FOR ST. JOHN'S WORT EXTRACT: PRELIMINARY STUDIES

Yoana Sotirova¹, Stanila Stoeva², Rositsa Nikolova³, Velichka Andonova¹

1) Department of Pharmaceutical Technologies, Faculty of Pharmacy, Medical University of Varna, Bulgaria.

2) Department of Pharmacology, Toxicology, and Pharmacotherapy, Faculty of Pharmacy, Medical University of Varna, Bulgaria.

3) Institute of Mineralogy and Crystallography, Bulgarian Academy of Sciences, Sofia, Bulgaria.

ABSTRACT:

Purpose: Nanostructured lipid carriers (NLC) can improve the stability of various phytochemicals, so this research aimed to develop and employ such delivery systems for *Hypericum perforatum* extract containing the light- and oxygen-sensitive phloroglucinol hyperforin.

Materials and methods: By varying the processing parameters and the solid and liquid lipids used, different NLC models were obtained via emulsification, followed by high-shear homogenization and ultrasonication. After characterization of the elaborated nanocarriers, those that exhibited optimal properties were loaded with St. John's wort extract by incorporating it in the lipid phase before emulsification and also studied.

Results: The NLC models developed by prolonged ultrasonication demonstrated favorable characteristics regarding particle size, polydispersity index (PDI), and zeta potential (ZP). The physically stable during long-term storage nanosystems, which also showed a reduced degree of crystallinity of the solid lipid included, were loaded with St. John's wort extract. Of the carriers so-obtained, those developed by ultrasonication at ambient temperatures can be described as acceptably uniform systems (PDI from 0.23 ± 0.01 to 0.27 ± 0.01), comprising particles with dimensions below 200 nm, favorable ZP values ($\zeta > |30 \text{ mV}|$), and superior entrapment efficacy (EE) greater than 85%.

Conclusion: In this research, different stable NLC dispersions were successfully developed. After the inclusion of the St. John's wort extract, the model possessing the highest EE ($87.77 \pm 0.64\%$) was chosen as a carrier to conduct further studies evaluating its wound-healing potential.

Keywords: lipid nanoparticles, *Hypericum perforatum*, physicochemical characterization,

INTRODUCTION

Nanostructured lipid carriers (NLC) are non-toxic, biocompatible, and biodegradable colloidal drug carriers mainly composed of lipid core and surfactant shell. Referred to as second generation after solid lipid nanoparticles, whose inner matrix is only built by solid lipids at ambient and physiological temperatures, they also contain variable amounts of liquid lipids. The addition of oils (fixed, essential, or semi-synthetic) achieves reduced crystallinity of the solid lipid included and, therefore, determines the capacity to entrap higher amounts of active principles and limits the rapid expulsion of the latter [1].

The thus-described lipid nanostructures have been extensively exploited to increase the stability of active pharmaceutical ingredients susceptible to environmental influences – from synthetic molecules such as tretinoin [2] to naturally-derived compounds including thymol, fucosanthin, and lutein [3 - 5]. Another biologically active substance sensitive to external factors (e.g., light and oxygen) is hyperforin – the main polyprenylated phloroglucinol in St. John's wort [6]. This phytochemical's antioxidant and antibacterial properties, combined with its ability to promote keratinocyte differentiation [7], define it as a suitable compound for wound treatment. Prior to its topical application, inclusion in a suitable drug delivery system is necessary for providing its stability. On the ground of hyperforin's lipophilic nature ($\log P = 13.17$) [8], utilizing NLC as a protective reservoir can be a reasonable approach for this aim.

With regard to dermal drug delivery, the selection of NLC structural components with a natural origin is preferable due to their similarity with the dermal lipophilic constituents, providing improved skin penetration and hydration [9]. As a well-known health-supporting liquid lipid, almond oil (AO) is considered beneficial in skin dryness due to its ability to reduce abnormal transepidermal water loss, rendering a moisturizing effect [10]. Another representative, already introduced in dermatological conditions such as seborrheic and atopic dermatitis, is borage oil –

one of the primary sources of gamma-linolenic acid [11,12]. Among solid lipids, beeswax (BW) can be considered eligible for topical NLC formulations due to the presence of small amounts of different antimicrobial compounds and vitamin A in its composition [13]. On the other hand, despite its synthetic origin, glyceryl behenate (GB) stands out as a complex glyceride with a less-defined structure providing superior drug encapsulation capability [14].

This study aimed to develop a physically stable NLC system, based on the lipids mentioned above, to serve as a potential carrier for St. John's wort extract, providing stability for subsequent dermal application.

MATERIALS AND METHODS:

Materials

All materials used in the study, including BW (Chemax Pharma, Bulgaria), BO (Alteya Organics, Bulgaria), AO (Alteya Organics, Bulgaria), polyoxyethylene (20) sorbitan monooleate (Tween® 80, Sigma-Aldrich, USA; SO), sorbitan monooleate (Span® 80, Sigma-Aldrich, USA; SM), and double-distilled water (Gesellschaft für Labortechnik GmbH, Germany; DDW) were of pharmaceutical grade. GB (Compritol® ATO 888) was kindly donated by Gattefossé, France.

Methods

Development and characterization of NLC dispersions

Preparation of the nanocarriers

NLC dispersions were prepared according to the described by Soleimanian et al. combination of techniques with a slight modification [15]. The lipid phase concentration was kept at 10% (w/w), with a solid: liquid lipid ratio of 7:3, and a constant amount of surfactant blend (5%, w/w), composed of 60% SM and 40% SO, was used. The influence of combining different solid and liquid lipids and varying the processing parameters on the NLC characteristics was investigated.

The lipid phase, containing solid and liquid lipids, and hydrophobic surfactant, was heated to $80\pm 2^\circ\text{C}$. Next, the aqueous phase (DDW and hydrophilic surfactant) was heated to the same temperature and added to the lipid phase dropwise under constant stirring at 750 rpm with IKA® RCT basic (IKA®-Werke, Staufen, Germany). After the latter, the resulting macroemulsion was stirred for 3 min while maintaining the elevated temperature. Subsequently, it was homogenized using an Ultra-Turrax® T25 high-speed disperser (IKA®-Werke, Staufen, Germany) for 3 min and placed in a sonication bath (Advantage-Lab™, Fisher Scientific GmbH, Austria) according to Table 1.

Table 1. Composition of the NLC models and processing parameters applied for their preparation.

Sample	Lipid phase, 10% (w/w)				Surfactants, 5% (w/w)		Aqueous phase, 85% (w/w)	High-shear homogenization speed, rpm	Ultrasoundication time, min	Temperature of ultrasoundication bath, °C
	Solid lipid, % (w/w)		Liquid lipid, % (w/w)		SM, % (w/w)	SO, % (w/w)	DDW, % (w/w)			
	BW	GB	AO	BO						
NLC1	70		30		60	40	100	10 000	15	25
NLC2	70			30	60	40	100	10 000	15	25
NLC3		70	30		60	40	100	10 000	15	25
NLC4		70		30	60	40	100	10 000	15	25
NLC5	70		30		60	40	100	10 000	15	4
NLC6	70			30	60	40	100	10 000	15	4
NLC7		70	30		60	40	100	10 000	15	4
NLC8		70		30	60	40	100	10 000	15	4
NLC9	70		30		60	40	100	10 000	5	25
NLC10	70			30	60	40	100	10 000	5	25
NLC11		70	30		60	40	100	10 000	5	25
NLC12		70		30	60	40	100	10 000	5	25
NLC13	70		30		60	40	100	10 000	5	4
NLC14	70			30	60	40	100	10 000	5	4
NLC15		70	30		60	40	100	10 000	5	4
NLC16		70		30	60	40	100	10 000	5	4
NLC17	70		30		60	40	100	15 000	-	-
NLC18	70			30	60	40	100	15 000	-	-
NLC19		70	30		60	40	100	15 000	-	-
NLC20		70		30	60	40	100	15 000	-	-

Particle size, polydispersity index, and zeta potential

The mean size (Z-average) and the polydispersity index (PDI) of the developed nanoparticles were investigated by dynamic light scattering (DLS) analysis. These parameters were evaluated at 25°C using Zetasizer Ultra (Malvern Panalytical Ltd., Malvern, UK), equipped with He-Ne laser operating at 633 nm. The measurements were performed in triplicate at a back-scattering angle of 173° after all colloidal dispersions were diluted 1000-fold in DDW to avoid multi-scattering phenomena. The zeta potential (ZP) values were assessed at 25°C via electrophoretic light scattering (ELS) using Zetasizer Ultra (Malvern Panalytical Ltd., Malvern, UK). Again, the samples were diluted by the factor of 1000 to obtain a suitable measurement density and analyzed in triplicate. All results obtained were expressed as mean ± standard deviation (SD).

X-ray diffraction studies

The initial solid lipids, the binary lipophilic mixtures (solid: liquid lipid in 7:3 ratios; BLM), and the developed NLC samples were analyzed by X-ray diffraction (XRD) using Panalytical Empyrean diffractometer (Malvern Panalytical Ltd., Malvern, UK). The measurements were carried out using Cu-K α radiation ($\lambda = 1.5406 \text{ \AA}$) in the two-theta range of 2-90° with a 1 s/step scanning rate and step size of 0.013°.

Storage stability

In order to investigate the physical stability of the NLC dispersions, they were visually observed for a possible formation of aggregates or gelling phenomenon. They were stored at 4°C for 6 months and inspected at time intervals of 1 month.

Development and physicochemical characterization of St. John's wort methanol extract-loaded NLC

Preparation of the colloidal systems

The selected NLC models were loaded with St. John's wort methanol extract (25% v/w from the weight of the lipid phase) by incorporating it into the lipophilic mixture before the emulsification step.

The extract was obtained via Soxhlet extraction by a previously described methodology. Hyperforin content (4.27 mg/mL) was quantified via the developed high-performance liquid chromatography with UV detection (HPLC-UV) method with isocratic elution of 0.3% phosphoric acid and acetonitrile (10/90, v/v) and limit of quantitation of 1.0 $\mu\text{g/mL}$ [16].

Particles' dimensions, surface electrical charge, and entrapment efficiency

In order to determine the particle size, PDI, and ZP of the *Hypericum perforatum* extract-loaded NLC suspensions (HP-NLC), the same procedures as described for the blank dispersions were followed.

The nanocarriers' entrapment efficiency (EE) was evaluated after the following steps: about 1 mL of the samples was centrifuged at 10 000 rpm for 10 min (D2012

Plus, DLAB Scientific, USA), subsequently filtered through Minisart® RC25 syringe filter with a 0.20 μm pore size (Sartorius, Goettingen, Germany), and diluted 1000-fold in DDW. The quantitative analysis was based on the above-mentioned HPLC-UV method, and the EE values were calculated from the following equation:

$$EE, \% = \frac{W_{\text{total hyperforin}} - W_{\text{free hyperforin}}}{W_{\text{total hyperforin}}} \cdot 100 \quad (\text{Eq. 1})$$

Where $W_{\text{total hyperforin}}$ is the amount of hyperforin included in NLC, and $W_{\text{free hyperforin}}$ represents the amount measured.

Transmission electron microscopy

The shape and structure of the optimal NLC and HP-NLC models were evaluated by transmission electron microscopy (TEM) using HRTEM JEOL JEM 2100 (JEOL Ltd. Japan) with an accelerating voltage of 200 kV. Before the observations, the nanosuspensions were gently homogenized by shaking for 30 s, subsequently dripped on a carbon-coated standard Cu grid, and air-dried in a dust-free environment for 24 h.

RESULTS AND DISCUSSION:

Characterization of NLC dispersions

Physical appearance

In this study, melt emulsification, high-shear homogenization, and ultrasonication were exploited to obtain nanosized lipid particles. This association of methods was employed, assuming that high-speed stirring produces micrometer-sized carriers and ultrasonication reduces their dimensions to the nanometer range [17].

The thus prepared NLC formulations (NLC1-NLC16) were slightly viscous, homogenous, milky-white liquids. A foam formation was reported when the high-shear homogenization step was carried out at 15 000 rpm (NLC17-NLC20), confirming that selecting an optimal shear intensity is crucial for preparing a stable dispersion [18]. Since the foaming employs surfactant molecules to reduce the air-liquid interface tension [19], the occurrence of this phenomenon may increase the physical instability of NLC dispersions in terms of coalescence or phase separation. Therefore, further studies on the nanoparticles' physicochemical properties were conducted on the first sixteen samples.

Particle size, degree of polydispersity, and ZP

DLS is a non-invasive technique widely used for particle size and particle size distribution analysis. Via measuring the velocity of the Brownian motion and converting it into a translational diffusion coefficient, the hydrodynamic diameter of the particles is calculated by the Einstein-Stokes equation:

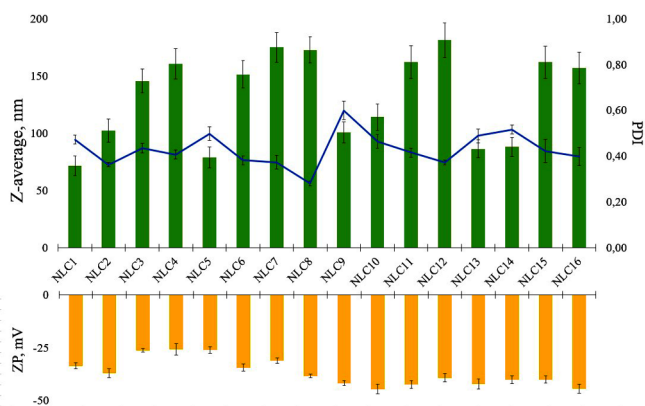
$$d_h = \frac{kT}{3\pi\eta D} \quad (\text{Eq. 2})$$

Where d_h is the hydrodynamic diameter, k is Boltzmann's constant, T is absolute temperature, η is viscosity, and D is diffusion coefficient. A typical representation of the DLS data obtained in terms of particles' dimensions is the intensity-weighted mean size (Z-average) [20].

PDI is a parameter used to describe the width of particle size distribution, as well as the uniformity of NLC suspensions and their proneness to aggregation. Monodisperse systems generally display a PDI of nearly 0, and the maximum value of 1 is distinctive for dispersions with highly various-sized particles. Typically, a PDI of less than 0.3 is preferred, but values lower than 0.5 can also be considered acceptable [21].

DLS results (fig. 1) demonstrated that all NLC suspensions possessed particles with mean size in the nano range below 200 nm, expressed as Z-average. The models containing BW as a solid lipid represented particles with smaller dimensions than GB-based ones. A possible explanation of these results, previously proposed by Soleimanian et al., can be the higher melting point of GB, determining the formation of a more viscous lipid phase [15]. Moreover, all elaborated nanoparticulate dispersions, excluding NLC9, showed PDI equal to or less than 0.5, and only NLC8 exhibited a lower than 0.3 value.

Fig. 1. Mean particle size, distribution width, and zeta potential of NLC dispersions (mean±SD).



ZP, the potential at the slipping plane of moving under an electrical field particle, is another characteristic associated with the stability of colloidal systems. Among applicable methods for its evaluation, ELS stands out as a precise and susceptible technique [22]. This analysis is based on the measurement of particles' mean electrophoretic mobility in suspension and consequently converting the values to zeta potential by Helmholtz–Smoluchowski equation:

$$\zeta = \frac{4\mu\pi\eta}{\epsilon} \quad (\text{Eq. 3})$$

Where μ is the electrophoretic mobility, η is the medium viscosity, and ϵ is the dielectric constant. According to ZP values, colloidal systems can be classified as highly unstable (± 0 – 10 mV), relatively stable (± 10 – 20 mV), moderately stable (± 20 – 30 mV), and highly stable (± 30 mV) [23].

All nanosized formulations possessed ZP values ranging from -25.64 ± 2.7 mV to -44.58 ± 2.2 mV (Figure 1). As the surfactants used are non-ionic, the negative charge on the nanoparticles' surface is probably due to the presence of acidic groups in GB [24], as well as free hydroxyl groups and fatty acids in BW [25].

All developed nanosuspensions can be characterized with high stability regarding the previously mentioned classification, excluding NLC1, NLC7, and NLC8, which can be considered moderately stable. However, the employed non-ionic surfactants (i.e., SM, SO) exert a steric repulsion effect, and the required minimum zeta potential in such cases is ± 20 mV [26]; therefore, the models above are also expected to remain stable.

When considering the influence of the variable processing conditions, it can be assumed that only the ultrasonication duration affected the parameters studied. The mean particle size was not altered, but the formation of more heterogeneous dispersions can be observed through higher PDI values. Therefore, models from NLC9 to NLC16 were discarded from the study, although they demonstrated higher ZP values.

Crystallinity studies

XRD is a nondestructive technique based on detecting the diffraction beam produced by an interaction of monochromatic X-rays with the crystalline lattice of a substance. In the pharmaceutical industry, it is widely utilized for quantifying the degree of crystallinity of various compounds, as well as different polymorphs identification, via transforming the acquired reflections to interlayer atomic spacings (d) using Bragg's equation:

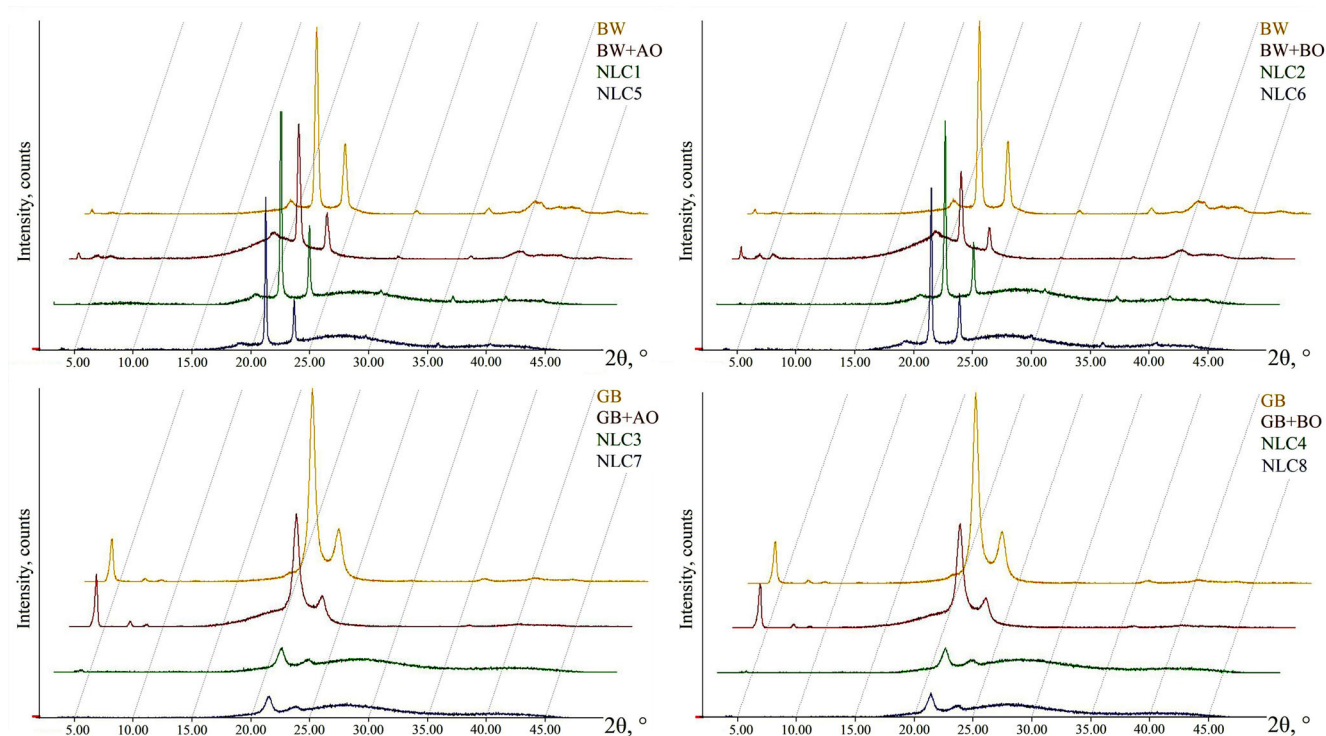
$$2d\sin\theta = n\lambda \quad (\text{Eq. 4})$$

Where θ is the diffraction angle, n is the order of the crystalline plane, and λ is the wavelength of the X-rays [27].

XRD studies were performed in order to explore the influence of the liquid lipid addition on the solid lipids' crystalline lattice, as well as the nanoparticles' structural order. It is common knowledge that obtaining nanoparticles with at least a partially disorganized structure can provide a higher capacity for drug encapsulation and reduce the possibility of rapid expulsion [1].

Diffraction patterns (with a given two-theta interval of 2 – 50°) of the solid lipids, BLM, and NLC suspensions are given in Fig. 2.

Fig. 2. Diffractograms of solid lipids, binary lipid mixtures, and NLC suspensions.



BW displayed low-intensity reflections at $2\theta=2.62^\circ$ ($d=3.37$ nm) and $2\theta=19.56^\circ$ ($d=0.45$ nm), representing the monoclinic structure of diesters, and the triclinic-orthorhombic polymorphs, resp [15, 28]. The high-intensity sharp peaks observed at $2\theta=21.74^\circ$ ($d=0.41$ nm) and $2\theta=24.14^\circ$ ($d=0.37$ nm) can be related to orthorhombic-arranged lattices of the hydrocarbons and monoesters (β' polymorphs) [28, 29]. GB showed three major reflexes at $2\theta=4.31^\circ$ ($d=2.05$ nm), $2\theta=21.37^\circ$ ($d=0.42$ nm), and $2\theta=23.59^\circ$ ($d=0.38$ nm), contributing to its orthorhombic β' polymorphic form [30].

The characteristic peaks of both BW and GB were broader and weaker in the BLM, indicating a reduced crystallinity, presumably related to the addition of the AO/BO. The d-spacing values of solid lipids remained unchanged, indicating the lack of polymorphic transitions after the oil addition or during the NLC preparation. Therefore, no rapid expulsion of a drug entrapped in these colloidal structures

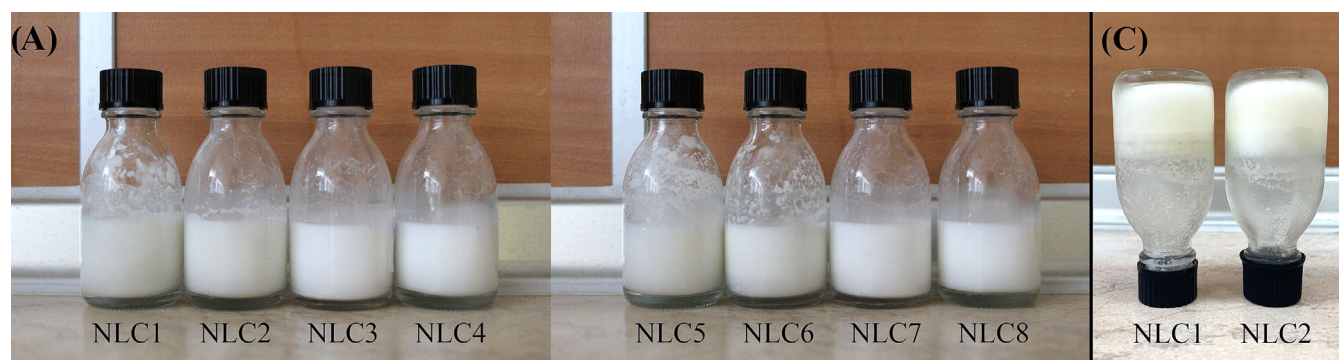
due to an altered crystal order could be expected [31].

A significantly reduced intensity of the main reflections was detected only in GB-containing NLC suspensions, referring to the less-ordered structure of the nanoparticles [32]. Moreover, no difference between the samples obtained at different ultrasonication temperatures was observed; therefore, it can be concluded that this variable operating parameter does not influence the order-disorder transitions.

Physical stability during storage

Maintaining the initial physicochemical properties of the colloidal particles is of great importance for their long-term stability. Besides aggregation and phase separation, gelation is another common process that can appear during the storage of NLC aqueous dispersion [33]. It is reported to occur when a polymorphic transition of the solid lipid is present, as well as when nanoparticles connect by lipid bridges and form a network [34, 35].

Fig. 3. Physical appearance of NLC dispersions immediately after preparation (A), after 1 month of storage at 4°C (B), and gel formation confirmation (C).





After a month of storage, the NLC samples containing BW as a solid lipid demonstrated phase separation and a subsequent gel formation after six months (fig. 3). Since the XRD studies did not show polymorphic changes, gelation is probably due to an insufficient uniformity of these systems – different-sized particles tend to aggregate easier [36], possibly promoting the lipid connections between them. Considering the development of physically stable NLC dispersions, BW-based nanosuspensions were excluded from the study. Further investigations were conducted only

with the colloidal systems based on GB, which remained stable during the observation period.

Physicochemical characterization of HP-NLC dispersions

Particle size, polydispersity index, zeta potential, and encapsulation efficiency

In order to assess the influence of the liquid extract addition on the particles' dimensions, their size distribution, and ZP, DLS and ELS studies were performed on all HP-NLC samples, and the results are represented in Table 2.

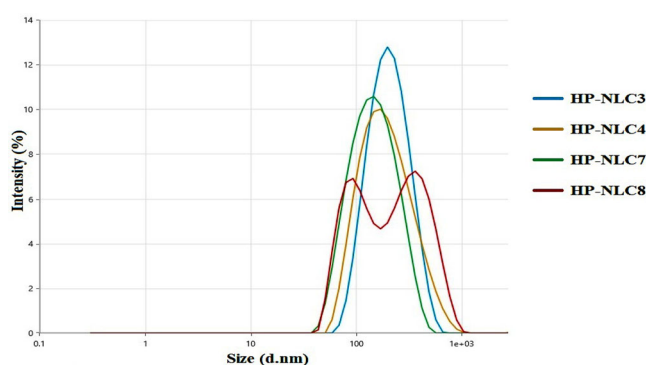
Table 2. Mean particle size, PDI, ZP, and EE of HP-NLC dispersions (mean±SD).

Sample	Z-average, nm	PDI	ZP, mV	EE, %
HP-NLC3	175.7±13.1	0.23±0.01	-41.11±0.7	85.25±0.82
HP-NLC4	175.9±8.9	0.27±0.01	-37.47±1.2	87.77±0.64
HP-NLC7	140.7±10.5	0.35±0.03	-44.21±2.0	82.79±0.51
HP-NLC8	158.1±9.2	0.31±0.02	-41.96±1.8	86.71±1.03

From the values obtained can be concluded that the entrapment of the extract did not alter the mean particle size of the carriers. Excluding HP-NLC4, where no change was observed, ZP values of the other HP-NLC samples were elevated compared to the corresponding NLC.

The size distributions of the four colloidal dispersions are given in fig. 4. The nanosuspensions produced by ultrasonication at ambient temperatures, as well as HP-NLC7, can be characterized as monodisperse systems. Conversely, HP-NLC8 displayed a bimodal distribution with clearly distinguished peaks at 92.89 nm and 361.3 nm resp.

Fig. 4. Size distribution by intensity of GB-based HP-NLC samples.

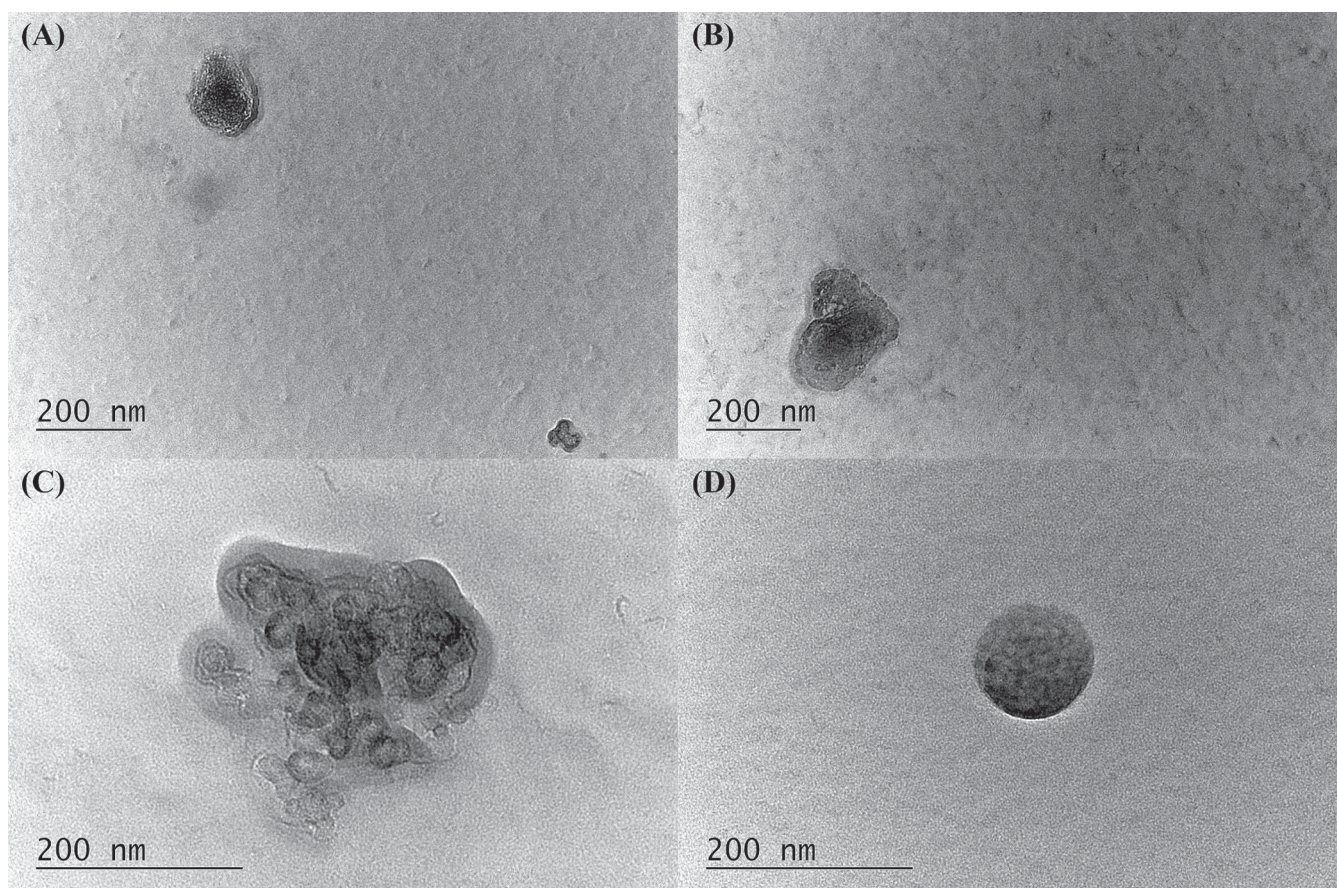


Another crucial feature of NLC is their ability to ensnare active substances, commonly measured via EE. Usually, values of about 60% and above suggest a prosperous preparation concerning drug incorporation [37]. All nanocarriers obtained showed excellent encapsulation capacities by means of high EE% values greater than 80%. Again, the influence of the ultrasonication temperature was emphasized – HP-NLC3 and HP-NLC4 entrapped higher amounts of the extract. Considering these results, as well as the degree of uniformity, the systems produced at 4°C were not further characterized.

Morphology studies

TEM is a long-established optical technique providing two-dimensional images and details about the internal structure of a sample investigated via an electron beam passing through it [20]. Besides the latter described, TEM analysis was carried out to confirm the colloidal sizes of the elaborated blank and extract-loaded nanosystems as well.

Fig. 5. TEM images of NLC3 (A), HP-NLC3 (B), NLC4 (C), and HP-NLC4 (D).



TEM observations were in accordance with DLS analysis for both blank and extract-loaded dispersions regarding nano-ranged mean particle size (fig. 5). According to the microphotographs, NLC3 can be assigned to the amorphous type of nanocarriers, while NLC4 revealed an imperfect crystal structure with well-delimited solid lipid grains. After incorporating the St. John's wort extract, there was no visible change in the inner morphology of GB/AO-based nanoparticles, but HP-NLC4 exhibited a more uniform architecture. Since no increase in the mean size of the latter was observed when compared to the corresponding blank carriers, the active principle was presumably incorporated into the gaps between the solid lipid fragments.

CONCLUSION:

In this study, different NLC models were developed by emulsification, high-speed homogenization, and ultrasonication, and the influence of the lipid constituents and operating parameters utilized was explored. The stirring speed altered the nanosuspensions' stability, and the duration of ultrasonication affected only the particle size distribution – the longer this preparation step, the more uniform the dispersion, regardless of the temperature maintained. The initial polymorphic modification of the solid lipids remained unchanged through the preparation process; however, the addition of a liquid lipid did not reduce the crystal order only in BW-based nanosystems. The latter exhibited gel formation during 6-month storage at 4°C,

vis-a-vis the GB-containing formulations, which remained physically stable. After incorporating the St. John's wort extract in the lipid phase prior to emulsification, the influence of the ultrasonication temperature was clarified by the higher EE values of HP-NLC3 and HP-NLC4. The model showing the highest encapsulation capacity, i.e., HP-NLC4, was chosen as a potential nano-reservoir for St. John's wort extract to further conduct *in vitro* release studies and evaluate its therapeutic potential in wound management *in vivo* after inclusion in a suitable semi-solid dosage form.

Abbreviations:

AO - Almond oil
BLM - Binary lipid mixtures
BO - Borage oil
BW - Beeswax
DDW - Double-distilled water
DLS - Dynamic light scattering
EE - Entrapment efficiency
ELS - Electrophoretic light scattering
GB - Glyceryl behenate
HP-NLC - Hypericum perforatum extract-loaded nanostructured lipid carriers
HPLC-UV - High-Performance Liquid Chromatography with UV detection
NLC - Nanostructured lipid carriers
PDI - Polydispersity index
SM - Sorbitan monooleate

SO - Polyoxyethylene (20) sorbitan monooleate
TEM - Transmission electron microscopy
XRD - X-ray diffraction
ZP - Zeta potential

Acknowledgements:

This work was funded by Medical University of Varna, Fund "Nauka" Project No. 18027.

REFERENCES:

1. D'Souza AA, Ranjita Shegokar R. Potential of oils in development of nanostructured lipid carriers. In: Essential Oils and Nanotechnology for Treatment of Microbial Diseases. Edited by Rai M, Zacchino S, Derita M. 1st Edition. CRC Press. 9 October 2017. Chapter 12, p. 242-257. [\[Crossref\]](#)
2. Chinsriwongkul A, Chareanputtakhun P, Ngawhirunpat T, Rojanarata T, Sila-on W, Ruktanonchai U, et al. Nanostructured lipid carriers (NLC) for parenteral delivery of an anticancer drug. *AAPS PharmSciTech*. 2012 Mar;13(1):150-158. [\[Crossref\]](#)
3. Pivetta TP, Simões S, Araujo MM, Carvalho T, Arruda C, Marcato, PD. Development of nanoparticles from natural lipids for topical delivery of thymol: Investigation of its anti-inflammatory properties. *Colloids Surf B Biointerfaces*. 2018 Apr;164:281-290. [\[Crossref\]](#)
4. Cordenonsi LM, Santer A, Sponchiado RM, Wingert NR, Raffin RP, Schapoval EES. Amazonia Products in Novel Lipid Nanoparticles for Fucoxanthin Encapsulation. *AAPS Pharm Sci Tech*. 2019 Dec;21(1):32. [\[Crossref\]](#)
5. Mitri K, Shegokar R, Gohla S, Anselmi C, Müller RH. Lipid nanocarriers for dermal delivery of lutein: Preparation, characterization, stability and performance. *Int J Pharm*. 2011 Jul 29;414(1-2):267-75. [\[PubMed\]](#)
6. Benzie IFF, Sissi Wachtel-Galor S. Medical Attributes of St. John's Wort (*Hypericum perforatum*). In: Herbal Medicine. Biomolecular and Clinical Aspects, Second Edition. Edited By Benzie IFF, Wachtel-Galor S. 2nd Edition. CRC Press. 2 May 2011. Chapter 11, p. 211-237. [\[Crossref\]](#)
7. Wölfle U, Seelinger G, Schempp C. Topical Application of St. John's Wort (*Hypericum perforatum*). *Planta Med*. 2014 Feb;80(2-3):109-120. [\[Crossref\]](#)
8. Gugleva V, Ivanova N, Sotirova Y, Andonova V. Dermal Drug Delivery of Phytochemicals with Phenolic Structure via Lipid-Based Nanotechnologies. *Pharmaceuticals (Basel)*. 2021 Aug;14(9):837. [\[Crossref\]](#)
9. Dobрева M, Stefanov S, Andonova V. Natural Lipids as Structural Components of Solid Lipid Nanoparticles and Nanostructured Lipid Carriers for Topical Delivery. *Curr Pharm Des*. 2020;26(36):4524-4535. [\[Crossref\]](#)
10. Blaak J, Staib P. An updated review on efficacy and benefits of sweet almond, evening primrose and jojoba oils in skin care applications. *Int J Cosmet Sci*. 2022 Feb;44(1):1-9. [\[Crossref\]](#)
11. Lin TK, Zhong L, Santiago JL. Anti-Inflammatory and Skin Barrier Repair Effects of Topical Application of Some Plant Oils. *Int J Mol Sci*. 2017 Dec 27;19(1):70. [\[PubMed\]](#)
12. Kanehara S, Ohtani T, Uede K, Furukawa F. Clinical effects of undershirts coated with borage oil on children with atopic dermatitis: a double-blind, placebo-controlled clinical trial. *J Dermatol*. 2007 Dec;34(12):811-815. [\[Crossref\]](#)
13. Kasparaviciene G, Savickas A, Kalvieniene Z, Velziene S, Kubiliene L, Bernatoniene J. Evaluation of Beeswax Influence on Physical Properties of Lipstick Using Instrumental and Sensory methods. *Evid Based Complement Altern Med*. 2016 Nov;2016:3816460. [\[Crossref\]](#)
14. Aburahma MH, Badr-Eldin SM. Compritol 888 ATO: a multifunctional lipid excipient in drug delivery systems and nanopharmaceuticals. *Expert Opin Drug Deliv*. 2014 Dec;11(12):1865-1883. [\[Crossref\]](#)
15. Soleimanian Y, Goli SAH, Varshosaz J, Sahafi, SM. Formulation and characterization of novel nanostructured lipid carriers made from beeswax, propolis wax and pomegranate seed oil. *Food Chem*. 2018 Apr;244:83-92. [\[Crossref\]](#)
16. Stefanov S, Stoeva S, Georgieva S, Hristova M, Nikolova K, Dobрева M, et al. *In vivo* comparative assessment of incised wound healing in rats after application of hydrogel/organogel formulation containing St. John's wort methanol extract. *Bulg Chem Commun*. 2022;54(B2):46-51. [\[Crossref\]](#)
17. Shimojo AAM, Fernandes ARV, Ferreira NRE, Sanchez-Lopez E, Santana MHA, Souto EB. Evaluation of the Influence of Process Parameters on the Properties of Resveratrol-Loaded NLC Using 22 Full Factorial Design. *Antioxidants (Basel)*. 2019 Aug;8(8):272. [\[Crossref\]](#)
18. Ashwani M, Sudheer P, Sogali BS. Custom design perspective in the process parameter optimization of nano lipid carriers. *Int J Appl Pharm*. 2020 Nov;12(6):198-208. [\[Crossref\]](#)
19. Dinache A, Pascu ML, Smarandache A. Spectral Properties of Foams and Emulsions. *Molecules*. 2021 Dec;26(24):7704. [\[Crossref\]](#)
20. Andonova V, Peneva P. Characterization Methods for Solid Lipid Nanoparticles (SLN) and Nanostructured Lipid Carriers (NLC). *Curr Pharm Des*. 2017 Nov;23(43):6630-6642. [\[Crossref\]](#)
21. Fernandes AV, Pydi CR, Verma R, Jose J, Kumar L. Design, preparation and in vitro characterizations of fluconazole loaded nanostructured lipid carriers. *Braz J Pharm Sci*. 2020 Mar;56:e18069. [\[Crossref\]](#)
22. Chen S, Dong H, Yang J. Surface Potential/Charge Sensing Techniques and Applications. *Sensors (Basel)*. 2020 Mar;20(6):1690. [\[Crossref\]](#)
23. Adegoke O, Park EY. Gold Nanoparticle-Quantum Dot Fluorescent

Nanohybrid: Application for Localized Surface Plasmon Resonance-induced Molecular Beacon Ultrasensitive DNA Detection. *Nanoscale Res Lett.* 2016 Nov;11:523. [[Crossref](#)]

24. Hassan DH, Shohdy JN, El-Setouhy DA, El-Nabarawi M, Naguib MJ. Compritol-Based Nanostructured Lipid Carriers (NLCs) for Augmentation of Zolmitriptan Bioavailability via the Transdermal Route: In Vitro Optimization, Ex Vivo Permeation, In Vivo Pharmacokinetic Study. *Pharmaceutics.* 2022 Jul;14(7):1484. [[Crossref](#)]

25. Thiruchenthooran V, Hvitalska M, Bonilla L, Espina M, García ML, Wietrzyk J, Sanchez-Lopez E, Gliszczynska A. Novel Strategies against Cancer: Dexibuprofen-Loaded Nanostructured Lipid Carriers. *Int J Mol Sci.* 2022 Oct;23(19):11310. [[Crossref](#)]

26. Zardini AA, Mohebbi M, Farhoosh R, Bolurian S. Production and characterization of nanostructured lipid carriers and solid lipid nanoparticles containing lycopene for food fortification. *J Food Sci Technol.* 2018 Jan;55(1):287-298. [[Crossref](#)]

27. Bunaciu AA, Udristioiu EG, Aboul-Enein HY. X-ray diffraction: instrumentation and applications. *Crit Rev Anal Chem.* 2015 May;45(4):289-299. [[Crossref](#)]

28. Gaillard Y, Mija A, Burr A, Darque-Ceretti E, Felder E, Sbirrazzuoli N. Green material composites from renewable resources: Polymorphic transitions and phase diagram of beeswax/rosin resin. *Thermochim Acta.* 2011 Jul;521(1–2):90-97. [[Crossref](#)]

29. Ensikat HJ, Boese M, Mader W, Barthlott W, Koch, K. Crystallinity of plant epicuticular waxes: electron and X-ray diffraction studies. *Chem Phys Lipids.* 2006 Oct;144(1):45-59. [[Crossref](#)]

30. Jennings V, Thünemann AF, Gohla SH. Characterization of a novel solid lipid nanoparticle carrier system based on binary mixtures of liquid and solid lipids. *Int J Pharm.* 2000 Apr;199(2):167-177. [[Crossref](#)]

31. Attama AA, Muller-Goymann CC. Effect of beeswax modification on the lipid matrix and solid lipid nanoparticle crystallinity. *Colloids Surf A Physicochem Eng Asp.* 2008 Feb;315(1–3):189-195. [[Crossref](#)]

32. Holder CF, Schaak RE. Tutorial on Powder X-ray Diffraction for characterizing nanoscale materials. *ACS Nano.* 2019 Jul;13(7):7359-7365. [[Crossref](#)]

33. Iordache T-A, Coc L, Mihai AL, Badea N, Lacatusu I, Meghea A. The Influence of Vegetable Oil and Self-organizing Agents' Composition on

Obtaining Stable Nanostructured Lipid Carriers. *UPB Sci Bull B Chem Mater Sci.* 2022 Mar;84(1):97-108. [[Internet](#)]

34. de Souza A, Yukuyama MN, Barbosa EJ, Monteiro LM, Faloppa ACB, Calixto LA, et al. A new medium-throughput screening design approach for the development of hydroxymethylnitrofurazone (NFOH) nanostructured lipid carrier for treating leishmaniasis. *Colloids Surf B Biointerfaces.* 2020 Sep;193:111097. [[Crossref](#)]

35. Cirri M, Maestrini L, Maestrelli F, Mennini N, Mura P, Ghelardini C, et al. Design, characterization and in vivo evaluation of nanostructured lipid carriers (NLC) as a new drug delivery system for hydrochlorothiazide oral administration in pediatric therapy. *Drug Deliv.* 2018 Nov;25(1):1910-1921. [[Crossref](#)]

36. Souto EB, Almeida AJ, Muller, RH. Lipid Nanoparticles (SLN®, NLC®) for Cutaneous Drug Delivery: Structure, Protection and Skin Effects. *J Biomed Nanotechnol.* 2007 Dec;3(4):317-331. [[Crossref](#)]

37. Haider M, Abdin SM, Kamal L, Orive G. Nanostructured Lipid Carriers for Delivery of Chemotherapeutics: A Review. *Pharmaceutics.* 2020 Mar;12(3):288. [[Crossref](#)]

Please cite this article as: Sotirova Y, Stoeva S, Nikolova R, Andonova V. Nanostructured Lipid Carriers as a Promising Dermal Delivery Platform for St. John's Wort Extract: Preliminary Studies. *J of IMAB.* 2023 Apr-Jun;29(2):4911-4919. [[Crossref](#) - <https://doi.org/10.5272/jimab.2023292.4911>]

Received: 03/01/2023; Published online: 09/05/2023



Address for correspondence:

Yoana Sotirova,
Department of Pharmaceutical Technologies, Medical University - Varna,
55, Marin Drinov Str., 9000 Varna, Bulgaria.
E-mail: Yoana.Sotirova@mu-varna.bg